J Therm Anal Calorim (2015) 120:1347–1354
DOI 10.1007/s10973-014-4378-y

Structural and thermal characteristics of Ni-doped carbosils prepared by mechanochemistry

Barbara Charmas

Received: 21 September 2014 / Accepted: 23 December 2014 / Published online: 29 January 2015

Abstract The paper presents the effects of differentiation of initial matrix (silica gel Si-50 or Aerosil A-200) and the addition of Ni^{2+} ions (in the form of $Ni(NO_3)_2 \cdot 6H_2O$) on structural and thermal properties of carbosils prepared by mechanochemical deposition of carbon matter (potato starch). Porous structure of the initial and modified materials was characterized by the low-temperature nitrogen adsorption/desorption method as well as by PSD calculated from the calorimetric data (DSC) using the thermal effects of phase transitions of water confined in carbosil pores. To evaluate comprehensive properties of the samples, the thermogravimetric (TG, DTG and DTA), spectroscopic (XRD, FTIR/ATR) and microscopic (SEM) investigations were carried out. It was found that mechanochemistry is an appropriate method for rebuilding the porous structure of silicas as well as for homogeneous deposition of carbon matter and catalyst on the silica matrices. It has been shown the nickel doping causes pore volume increase and lowering of carbon deposit thermal stability. The obtained carbosils are mesoporous materials with a small amount of micropores created in the carbon part.

Keywords Carbon–mineral adsorbents · Differential scanning calorimetry · Thermogravimetry · Porous structure

The present article is based on the lecture presented at ICVMTT 34 conference in Kyiv-Ukraine on 20–21 May, 2014.

B. Charmas (✉)
Department of Chromatographic Methods, Faculty of Chemistry, Maria Curie-Sklodowska University, Maria Curie-Sklodowska Sq. 3, 20–031 Lublin, Poland
e-mail: barbara.charmas@poczta.umcs.lublin.pl

Introduction

Rapid development of industry involves the need to intensify research on new porous materials preparation. Promising materials, due to the dual nature of the surface, are carbon–silica adsorbents (carbosils) [1, 2]. These hybrid materials combine characteristics of the non-polar carbon and polar mineral matrix, allowing adsorption of both polar and non-polar media [2–7]. Properties of carbosils can be controlled and monitored in the stage of preparation, by choosing appropriate mineral matrix, adjusting amount and chemical nature of carbon deposit precursors, different modification ways and/or catalyst addition. The preparation method is extremely important. In recent years, due to the increasing awareness of environmental problems, the increased interest in "clean methods," including mechanochemistry, has been observed. This unconventional method of preparation consists in conversion of mechanical energy formed during collisions of grinding balls in the heat allowing chemical reactions to proceed. The application of this method allowed the use of natural organic materials (e.g., starch) as a carbonaceous matter. Conditions created in the mechanochemical process (high temperature and pressure) were favorable for the starch gelation process while covering the silica matrix with carbon matter. In such conditions, one would expect that carbon deposit is a compact and homogeneous surface. However, it was shown [8] that the mechanism of carbon deposition depends on many factors and even with large contents of deposit, a hybrid material of a mosaic-like carbon structure is obtained and its topography can be considered as "patch-wise."

Different methods for characterization of surface properties of solid adsorbents have been proposed [9–12]. The aim of the paper was to study how differentiation of mineral matrix and catalyst content influence on porosity and

thermal stability of the obtained carbosils as well as to make their thorough characterization. In this study, the adsorption (N_2), calorimetric (DSC), thermal (TG), spectroscopic (XRD, ATR/FTIR) and microscopic (SEM) methods were applied. Knowledge of structural characteristics is necessary for these materials to be used in different practical areas.

Materials and methods

Preparation of adsorbents

Carbon–silica adsorbents were prepared on the basis of two types of siliceous materials: Sipernat 50 (porous silica gel, S-50, Degussa, Germany) and Aerosil 200 (fumed silica, non-porous, A-200, Kalush, Ukraine). The commercial potato starch (Superior, Poland) as a carbon source was used, while $Ni(NO_3)_2{\cdot}6H_2O$ (POCh, Poland) was Ni^{2+} ions' source. The initial carbosils without Ni and those doped with different amounts of nickel were prepared. The molar ratio of SiO_2/starch/Ni^{2+} was 1:0.3:0.1–0.5.

Preparation of the mixtures takes place using mechanochemistry as a method of carbonaceous matter and catalyst application. Mechanochemical treatment of prepared mixtures (Planetary Mill, PULVERISETTE 7, Fritsch, Germany) proceeded according to the following procedure: pre-grinding for 15 min, 500 rpm [grinding $Ni(NO_3)_2{\cdot}6H_2O$ and homogenization of the mixture], followed by grinding for 30 min (2 × 15 min), 750 rpm (heating of the system, resulting starch gelation and better homogenization of the sample). Additionally, to examine the effect of mechanochemical treatment on porous structure of the matrix, the initial silicas were subjected to mechanochemical treatment under the same conditions and they are denoted A-200 M and S-50 M.

All the silica/starch/$Ni(NO_3)_2$ mixtures obtained mechanochemically were subjected to the pyrolysis process. The pyrolysis was carried out in a rotary quartz reactor in nitrogen atmosphere (120 cm^3 min^{-1}) using the following procedure: heating from 20 to 500 °C (10 °C min^{-1}), isothermal annealing at 500 °C (3 h) and cooling to room temperature. The samples obtained in this way are denoted with the general formulae SS_{Ni-x} (for the samples prepared on the base of Sipernat) and AS_{Ni-x} (for the samples prepared on the base of Aerosil, where $x = 0, 0.1, \ldots, 0.5$).

N_2 adsorption

Nitrogen adsorption–desorption isotherms were recorded at −196 °C by means of a Micromeritics ASAP 2405 N adsorption analyzer. The specific surface area S_{BET} was calculated using the standard BET equation [13] at p/p_o between 0.06 and 0.2 (where p and p_o denote the equilibrium and saturation pressures of nitrogen, respectively). The pore volume V_p was estimated under the relative pressure $p/p_o \approx 0.98$. V_{mic} was determined using the t plot method. The average pore radius (R_{av}) was calculated for a model of cylindrical pores $R_{av} = 2V_p/S_{BET}$. Pore volume distributions in the function of their radii were calculated by using the Barrett–Joyner–Halenda (BJH) method [14].

Thermogravimetric analysis

The carbon content (C_C) and thermal stability of carbon deposit in carbosils were determined using the thermogravimetry (TG, DTG) and differential thermal analysis (DTA) by heating the samples in air atmosphere from 20 to 1,200 °C (Derivatograph C, Paulik, Paulik and Erdey, MOM, Hungary) at the heating rate of 10 °C min^{-1}.

DSC investigations

The curves of freezing/melting of the water confined in the carbosil pores were determined by differential scanning calorimetry (Diamond DSC, Perkin Elmer, USA). The test samples were initially saturated with water (ultrasonic bath, 5 min) and sealed into aluminum pans. As a control, an empty aluminum crucible was used. Measurements were carried out in an atmosphere of inert gas (helium). In order to prevent the system defrosting, nitrogen was used as the curtain gas. Experiments were performed at a rate of temperature change 2 °C min^{-1}. Ice melting inside the pores was determined in the temperature range from −50 to +20 °C. The obtained curves of ice melting were used to determine the temperature characteristic of the observed thermal effects (T_{max} and T_{onset}) and the PSD curves.

Thermoporometry DSC was used to examine phase transitions of water confined inside the pores. The ongoing study is based on the fact that in the pores of mesoporous materials there can be two types of water, i.e., water freezing in the pores (unbound or weakly bound to the surface of pores) and non-freezing water (strongly associated with the surface of pores). The DSC data of ice melting process were used to determine the size of water clusters formed on/within the pores of tested carbosils. Water in the narrowest pores freezes at lower temperature so shift of the thermal effects can be observed on the curves. In the studies, water in the pores of R_{min} is assumed to melt at T_{onset} (temperature of the phase transition start), while the temperature T_{max} (at which the rate of phase transition is the highest) corresponds to melting of water in R_{av} pores. The mathematical relationship is represented by the Gibbs–Thomson equation (GT), taking into account the correlation between the reduction in the freezing point of water inside the cylindrical pores and the pore size R_p [15–18]:

$$R_p/\mathrm{nm} = 0.68 - \frac{k_{GT}}{T_m - T_{m0}} \quad (1)$$

where T_m and T_{m0} are the temperatures of melting of ice contained in the pores in the bound and unbound forms, respectively, k_{GT}—the constant. The pore volume distribution curve (*PSD*) d*V*/d*R* was determined from the ice melting curve:

$$\frac{dV}{dR}(\mathrm{cm^3\,nm^{-1}\,g^{-1}}) = \frac{\frac{dq}{dt}(T_m - T_{m0})^2}{k_{GT}\rho\beta m\Delta H(T)} \quad (2)$$

where d*q*/d*t*, ρ, β, m and $\Delta H(T)$ are the heat flow, the water density, the rate of temperature change, the sample mass and the ice melting enthalpy, respectively. The ΔH dependence on the temperature can be calculated from the relationship:

$$\Delta H(T)[\mathrm{J\,g^{-1}}] = 332 + 11.39(T_m - T_{m0}) + 0.155(T_m - T_{m0})^2 \quad (3)$$

XRD

The powder X-ray diffractometer (HZG-4, Carl Zeiss Jena, Germany) was used to analyze the phase composition and crystallite sizes of carbosils. The scanning step was 0.03° (angle 2Θ), CuKα radiation, the measuring range 10–80°. The crystallite sizes were determined using the Scherrer's formula.

FTIR/ATR

FTIR investigations were performed using a microscope Nicolet iN10 MX (ThermoScientific). The IR spectra were registered by the ATR method with a germanium crystal directly from the sample surface in the wave number range 4,000–650 $\mathrm{cm^{-1}}$ using a MTC detector cooled with liquid nitrogen. The experiment was performed using the spectral resolving power 8 $\mathrm{cm^{-1}}$. The spectra were subjected to the baseline correction using the OmnicSpecta™ software.

SEM

Surface morphology (imaging) and nickel content (microanalysis) of the tested carbosils were examined using the most versatile high resolution, low-vacuum scanning electron microscope Quanta™ 3D FEG (FEI™ USA).

Results and discussion

Table 1 presents the porous structure characteristics of studied materials, and Fig. 1 shows the low-temperature nitrogen adsorption/desorption isotherms (Fig. 1a) as well as the curves of pore size distribution (Fig. 1b) for starting and mechanochemically modified silicas. The analysis of the course of isotherms and pore size distribution curves indicates that mechanochemical treatment of starting materials caused significant changes in their porous structure. A significant decrease in the specific surface area and pore volume (Table 1) of the samples A-200 M and S-50 M was observed. In the case of Sipernat, grinding caused a decrease in the specific surface area from 361 to 224 $\mathrm{m^2\,g^{-1}}$, while for Aerosil, the reduction in S_{BET} from 215 to 100 $\mathrm{m^2\,g^{-1}}$ was found. In both cases, an approximately 50 % decrease in pore volume was found. This results from the fact that mechanochemical modification of

Table 1 Structural characteristics of tested samples

Sample	S_{BET}/$\mathrm{m^2\,g^{-1}}$	S_{micro}/$\mathrm{m^2\,g^{-1}}$	V_p/$\mathrm{cm^3\,g^{-1}}$	V_{micro}/$\mathrm{cm^3\,g^{-1}}$	R_{av}/nm
S-50	361	32.8	1.23	0.01	6.80
S-50 M	224	21.3	0.53	0.01	4.80
A-200	215	13.1	0.43	0.00	4.05
A-200 M	100	1.8	0.20	0.00	4.00
SS_{Ni-0}	188	92.2	0.15	0.04	1.61
$SS_{Ni-0.1}$	232	101.9	0.17	0.04	1.50
$SS_{Ni-0.2}$	243	85.8	0.21	0.04	1.75
$SS_{Ni-0.3}$	250	88.2	0.24	0.04	1.89
$SS_{Ni-0.4}$	224	40.3	0.25	0.02	2.23
$SS_{Ni-0.5}$	246	41.3	0.30	0.02	2.42
AS_{Ni-0}	192	90.6	0.16	0.04	1.64
$AS_{Ni-0.1}$	237	69.8	0.20	0.03	1.67
$AS_{Ni-0.2}$	251	69.0	0.23	0.03	1.82
$AS_{Ni-0.3}$	221	51.7	0.23	0.02	2.06
$AS_{Ni-0.4}$	225	56.4	0.23	0.02	2.07
$AS_{Ni-0.5}$	213	43.3	0.26	0.02	2.40

porous silica (S-50) caused damage of rigid structure and destruction of pores thus decreasing the specific surface area and pores volume. In the case of fumed silica (A-200) due to the mechanochemical treatment, the globules loose structure was rearranged into a more compact one by destruction of void spaces among the SiO_2 nanoparticle aggregates decreasing the specific surface area and pores volume. The shape of the analyzed isotherms and the data

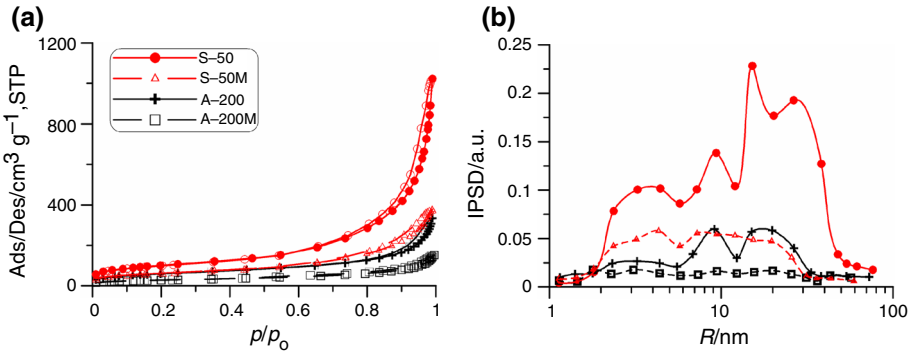

Fig. 1 Low-temperature nitrogen adsorption/desorption isotherms (**a**) and incremental pore size distribution curves (**b**) for starting and mechanochemically modified silicas

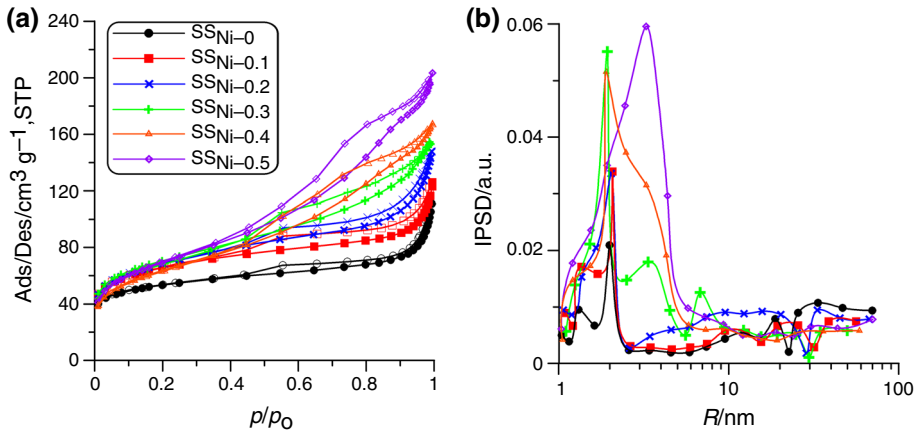

Fig. 2 Low-temperature nitrogen adsorption/desorption isotherms (**a**) and incremental pore size distribution curves (**b**) for SS carbosils series

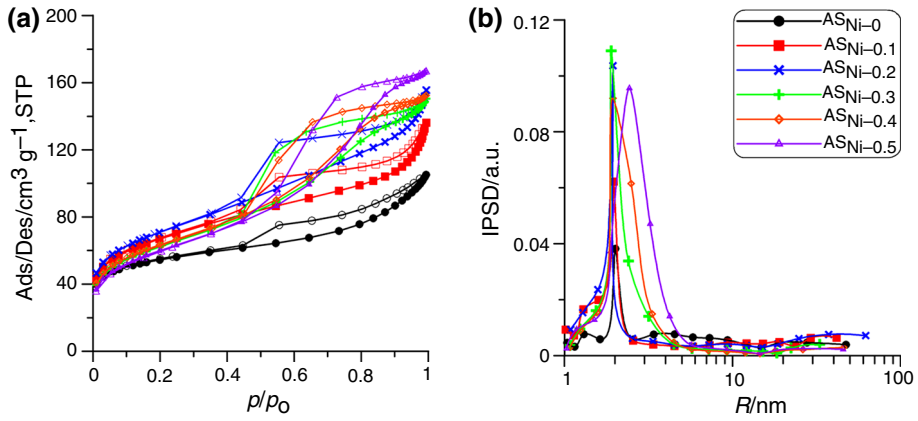

Fig. 3 Low-temperature nitrogen adsorption/desorption isotherms (**a**) and incremental pore size distribution curves (**b**) for AS carbosils series

included in Table 1 indicate that these are mesoporous materials (with a small amount of micropores, $S_{micro} \approx 10\ \% S_{BET}$) of poorly developed porous structure characterized by wide pore size distribution.

Figures 2 and 3 present the nitrogen adsorption/desorption isotherms and the PSD curves for the studied series of carbosils. The isotherms shape determined for all studied carbosils (except AS_{Ni-0} and SS_{Ni-0}) is typical of mesoporous adsorbents. Poorly formed hysteresis loops, which become more distinct with the increasing nickel content in individual samples, are observed. The shape of hysteresis loops (type H3 according to the IUPAC classification [13]) shows that these adsorbents possess open regular and irregular cylinders and prisms as well as slits with parallel wall-shaped pores. Carbon deposition on the silica matrices resulted in the decrease in specific surface area of the material prepared on the base of Sipernat (SS_{Ni-0}, Table 1) and the increase in S_{BET} of the material prepared on the base of Aerosil (AS_{Ni-0}, Table 1) compared to the corresponding starting materials, that is, S-50 M and A-200 M. This indicates a significant effect of starting silica and its modification on properties of the obtained carbon–silica materials. Decrease in the total volume of the pores V_p was observed for both samples (AS_{Ni-0} and SS_{Ni-0}, Table 1).

In the case of both series of Ni-doped carbosils (Figs. 2, 3), the nickel content increase resulted in the initial (lower nickel contents) increase in specific surface area. The largest S_{BET} value was determined for the $AS_{Ni-0.2}$ and $SS_{Ni-0.3}$ samples (Table 1). Further increase in the nickel content did not cause significant changes in the specific surface area. As follows from the PSD curves analysis, the studied adsorbents of the SS_{Ni-x} series are characterized by the presence of pores of various sizes of average radii R (Fig. 2b), but the adsorbents prepared on the base of Aerosil are characterized by homogeneous and narrow distribution of pore sizes of $R_{av} = 2$–3 nm (Fig. 3b). V_p and R_{av} increase with the increasing catalyst content in the series of adsorbents (Table 1). Moreover, in the studied materials, the structure of micropores (S_{micro}, V_{micro}, Table 1) was developed to a small extent. The analysis of

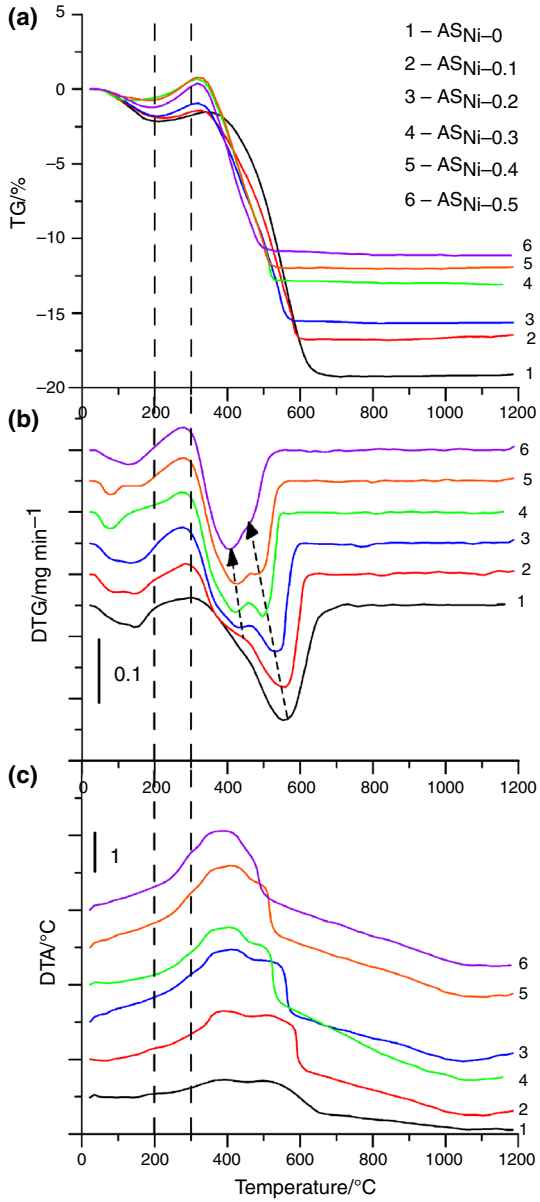

Fig. 4 TG (**a**), DTG (**b**) and DTA (**c**) curves for AS carbosils series

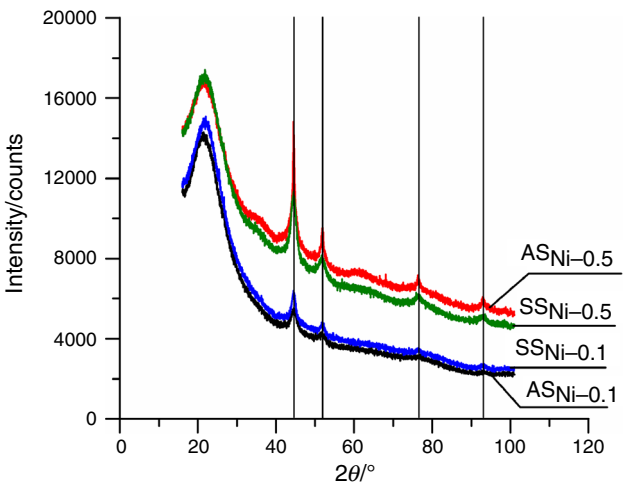

Fig. 5 XRD diffractograms for carbosils of minimal and maximal Ni contents

the data in Table 1 indicates that the micropores are created in the carbonaceous part of the tested materials because for the initial and mechanochemically treated silicas small micropore surfaces are observed. Moreover, increasing the catalyst amount reduces the possibility of creating micropores. With the increasing of catalyst, the micropores surface S_{micro} is reduced. This can be seen explicitly in each carbosils series.

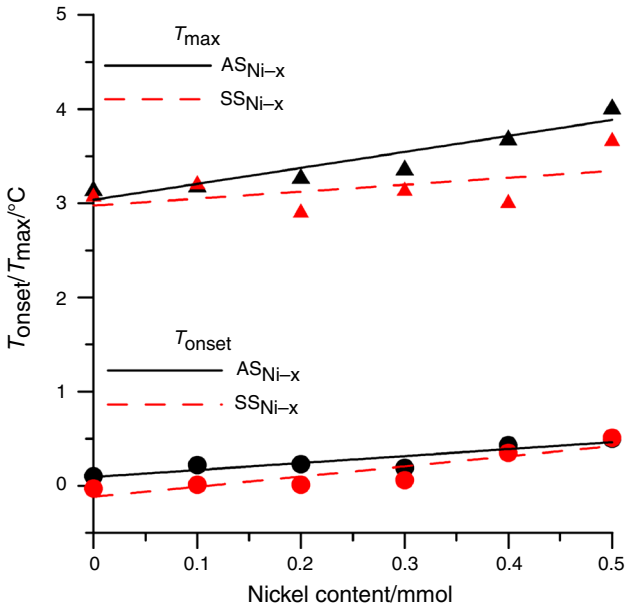

Fig. 6 Changes of T_{onset} and T_{max} depending of the Ni content

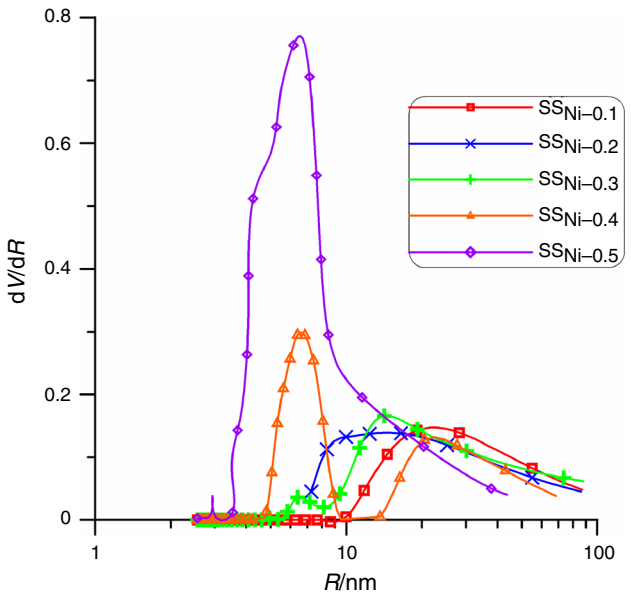

Fig. 7 Differential pore size distribution curves for SS_{Ni-x} carbosils series obtained from DSC curves

In order to estimate the content and determine thermal stability of carbon deposit of the samples, the thermogravimetric analysis was applied. During the analysis, there were registered the TG, DTG and DTA curves which are presented in Fig. 4, for example, for the AS_{Ni-x} series. The TG curves (Fig. 4a) indicate a two-stage process of mass loss. Small mass losses are observed up to 200 °C which is connected with desorption of physically bound water from the sample surfaces. This process can be seen on the DTG curves (Fig. 4b). As these changes are very small, this phenomenon is not observed on the DTA curves (Fig. 4c). In the temperature range about 200–400 °C, small maxima indicating the mass increase in the samples are observed on the curves. This is caused by the adsorption of oxygen from surrounding atmosphere on the surface. The increase is more intensive for the materials obtained on the base of Aerosil and extends with the increasing nickel content (Fig. 4a). Then, carbon deposit combustion starts at about 350 °C. The presence of nickel catalyzes the combustion process. The deposit in the samples of the largest content of catalyst starts combustion at the earliest. With the increasing nickel content, the temperature at which the process is the fastest (the minimum on the DTG curve, dotted lines, Fig. 4b) shifts toward lower values. For the sample without the addition of nickel (AS_{Ni-0}), combustion starts at over 400 °C, i.e., by 100 °C higher compared to the sample with the largest nickel content. Moreover, on the DTG curves of nickel-doped carbosils (Fig. 4b), two maxima can be seen. This is the evidence for the existence of carbon deposit of differentiated thermal stability because of nickel addition, which is confirmed by the analysis of complex DTA curves (Fig. 4c). The largest mass losses are

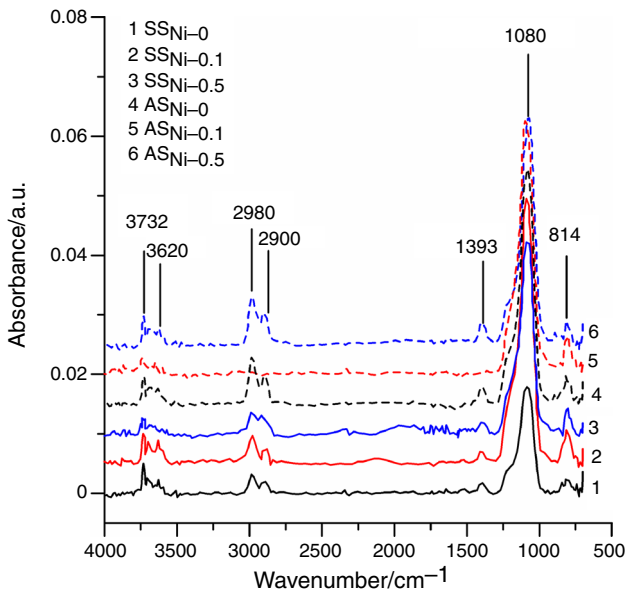

Fig. 8 ATR/FTIR spectra for selected samples of SS and AS series

found for the samples without the catalyst addition. The carbon deposit of these samples (AS_{Ni-0} and SS_{Ni-0}) burns up to 650 °C. The presence of nickel in the studied samples causes reduction in relative content of carbon deposit, and this tendency is maintained with the increasing catalyst content (Fig. 4a). In the studied materials, the deposit content changed from 11 to 19 %. In the case of all carbosils prepared on the base of Sipernat (not shown here), combustion of carbon deposit starts at about 315 °C independent of the presence and content of nickel. This is the evidence for the significant effect of the mineral matrix on the carbon deposit structure. A complex course of DTG and DTA curves is analogous to that for the samples prepared on the base of Aerosil (Fig. 4).

Due to possible adsorption on the carbosil surface, it was essential to determine form and size of nickel crystallites in the studied materials. Figure 5 presents the XRD diffractograms of carbosils of minimal and maximal contents of the catalyst. The XRD pattern contains reflexes indicating the existence of Ni in the metallic form. Since the grains contain crystalline domains, the crystallite sizes are much smaller than those of grains. In the tested samples, the crystallite sizes calculated from the Scherrer's equation are 5–17 nm.

To analyze chemical character of carbosils surface, the FTIR studies were made. The analysis of the FTIR/ATR spectra obtained for the carbosils shown in Fig. 6 gives evidence for the presence of both silica matrices ($\nu_{Si-O-Si}$: 814 and 1,080 cm^{-1}) and carbon deposit (ν_{-CH3}: 2,980 and 2,900 cm^{-1} as well as δ^{s}_{-CH3}: 1,393 cm^{-1}) as well as the bands characteristic of the surface hydroxyl groups (ν_{-OH}: 3,732 and 3,620 cm^{-1}). This confirms the incomplete coverage of the silica matrices by carbon deposit patches.

The DSC method was used for the analysis of phase transitions during the process of water freezing and ice melting in the studied materials. From the DSC curves, the depression of ice melting temperature (T_{onset}, T_{max}) was determined and the obtained data were used for determination of the PSD curves. The obtained curves of water freezing are of typical shape characteristic of porous materials. They are characterized by a complex course and possess minima (exothermic) indicating the existence of complex porous structure of the studied materials. Figure 7 presents the course of changes of the T_{onset} and T_{max} temperatures obtained from the curves of ice melting in the pores of studied adsorbents. As follows from the analysis of T_{onset} and T_{max} changes (Fig. 7), the above presented values shift toward a higher temperature with the increasing nickel content. This shift is due to the changes of porous structure parameters observed with the increasing nickel content in carbosils (Table 1). Figure 8 presents the exemplary PSD curves for the SS series. Generally, the increase in nickel content in the studied carbosils causes the shift of curve maxima toward higher values of R_{av}

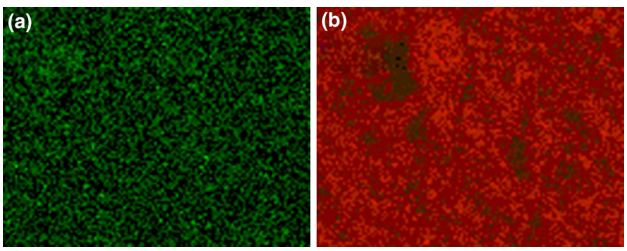

Fig. 9 SEM maps of the $SS_{Ni-0.5}$ surface including the distribution of nickel (**a**) and silicon (**b**)

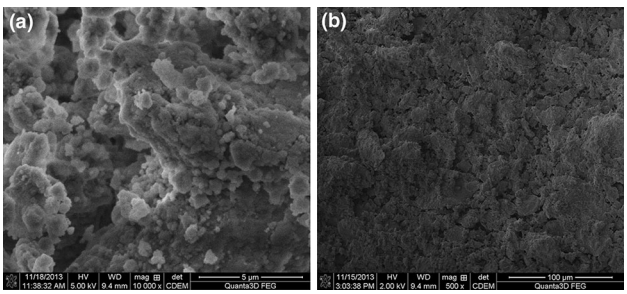

Fig. 10 SEM images of the $SS_{Ni-0.5}$ surface of ×10,000 (**a**) and ×500 (**b**) magnification

which indicates the increasing pore radii. This is consistent with the course of curves presented in Fig. 7 and R_{av} presented in Table 1.

Complementary information on the morphology of surface and nickel contents in the analyzed carbosils comes from the studies carried out by a scanning electron microscopy. Microanalysis performed by SEM showed that in the tested carbosils, there was from 7.5 to approx. 23 mass% Ni for the samples of nickel content from 0.1 to 0.5, respectively. Figure 9 presents the exemplary SEM maps of the $SS_{Ni-0.3}$ surface, including the distribution of nickel (Fig. 9a) and silicon (Fig. 9b). Mapping of the surface showed that nickel is distributed in the form of a uniform surface layer consisting of small crystallites which is consistent with the results obtained by XRD. Silicon distribution indicates the existence of surface irregularities and roughness, probably caused by mechanochemical pretreatment. Figure 10 shows the SEM images of $SS_{Ni-0.3}$ surface. The surface texture is varied (Fig. 10a, 20,000×), and the aggregates and agglomerates are of different sizes, causing the effect of "roughness." Smaller magnification (500×, Fig. 10b) indicates the existence of surface patches (probably carbon deposit) resulting in formation of pores of the shape of open regular and irregular cylinders and prisms as well as those of slits with parallel wall shape.

Conclusions

The study shows that mechanochemistry is a convenient method of homogeneous application of carbon matter and/or a catalyst on the surface of the mineral matrix to prepare the hybrid adsorbents. The mechanochemical treatment causes destruction of the compact matrix of porous silica and reconstruction of Aerosil structure, resulting in a significant reduction in the surface area and pore volume. The obtained carbosils have a developed specific surface area (188–250 $m^2\ g^{-1}$) and porous structure in the range of narrow pores. They also possess a small amount of micropores, created in the carbon part of material. On the surface, they contain active sites in the form of metallic nickel crystallites of 5–17 nm sizes. Surface heterogeneity also follows from the presence of surface hydroxyl groups, indicating incomplete coverage of silica surface with the carbon deposit. The increase in the nickel content causes the increase in pore volume and the reduction in thermal resistance of carbon deposit. The PSD curves obtained on the basis of DSC ones confirm the mesoporous structure of the prepared adsorbents, and they are consistent with the results obtained from the data of nitrogen adsorption/desorption isotherms.

References

1. Leboda R, Dąbrowski A. Complex carbon-mineral adsorbents: preparation, surface properties and their modification. In: Dąbrowski A, Tertykh VA, editors. Adsorption and chemisorption on inorganic sorbents. Amsterdam: Elsevier; 1996.
2. Gun'ko VM, Leboda R. Carbon-silica gel adsorbents. In: Hubbar AT, editor. Encyclopedia of surface and colloid science. New York: Marcel Dekker; 2002. p. 864.
3. Skubiszewska-Zięba J, Leboda R, Gun'ko VM, Charmas B. Structural and adsorption characteristics of pyrocarbon-mineral adsorbents. In: Blitz JP, Gun'ko VM, editors. Surface chemistry in biomedical and environmental science. NATO science series II: mathematics, physics and chemistry. Berlin: Springer; 2006. p. 123.
4. Leboda R, Turov VV, Charmas B, Skubiszewska-Zięba J, Gun'ko VM. Surface properties of mesoporous carbon–silica gel adsorbents. J Colloid Interface Sci. 2000;223:112–25.
5. Leboda R. Carbon-mineral adsorbents—new type of sorbents? Part I. The methods of preparation. Mater Chem Phys. 1992;31:234–55.
6. Leboda R. Carbon-mineral adsorbents—new type of sorbents part II. Surface properties and methods of their modification. Mater Chem Phys. 1993;34:123–41.
7. Kamegawa K, Yoshida H. Carbon coated of silica surface. I. Pyrolysis of silica gels esterified with alcohols. J Colloid Interface Sci. 1993;159:324–7.
8. Puziy AM, Charmas B, Poddubnaya OI, Mel'gunov MS, Leboda R, Trznadel BJ. Surface heterogeneity of carbon-silica adsorbents studied on the basis of the complex adsorption investigations. Colloids Surf A. 2003;213:45–57.
9. Jaroniec M, Madey R. Physical adsorption on heterogeneous solids. Amsterdam: Elsevier; 1988.
10. Rudziński W, Everett DH. Adsorption of gases on heterogeneous solids surface. New York: Academic Press; 1992.
11. Dekany I, Nagy LG. Liquid sorption and wetting oil hydrophilic/hydrophobic layer silicates. Colloids Surf. 1991;58:251–61.
12. Gunko VM, Turov VV. Nuclear magnetic resonance studies of interfacial phenomena. San Diego: Taylor & Francis; 2013.
13. Gregg SJ, Sing KSW. Adsorption, surface area and porosity. London: Academic Press; 1982.
14. Barrett EP, Joyner LG, Halenda PP. The determination of pore volume and area distributions in porous substances. I. Computations from nitrogen isotherms. J Am Chem Soc. 1951;73:373–80.
15. Brun M, Lallemand A, Quinson J, Eyraud C. A new method for the simultaneous determination of the size and the shape of pores. Thermochim Acta. 1977;21:59–88.
16. Landry MR. Thermoporometry by differential scanning calorimetry: experimental considerations and applications. Thermochim Acta. 2005;433:27–50.
17. Charmas B. Adsorption and calorimetric studies of hydrothermally modified carbosils. J Therm Anal Calorim. 2014;115:1395–405.
18. Weber J, Bergström L. Mesoporous hydrogels: revealing reversible porosity by cryoporometry, X-ray scattering, and gas adsorption. Langmuir. 2010;26:10158–64.